Gabriel Durazo
Aerospace Laboratory MMAE 315
November 17th, 2026

Analysis of a NACA 0012 Airfoil

Abstract

The foundation of this experiment and its analysis was the thin airfoil theory. The pressure, lift, and drag coefficient of a NACA 0012 symmetric airfoil, without camber, were observed as well as compared to published data. It was expected that the collected data would match the empirical data but it did not. The empirical data from Turbulence Modeling Resource showed that the $C_{L,max}$ was reached at an attack angle of 17° whereas the analyzed data showed that $C_{L,max}$ was reached at an attack angle of 15°. Past this point, the airfoil stalls resulting in a decrease of performance. Although the collected data and the empirical results showed different stalling points, the thin airfoil theory is still applicable with an attack angle in the range of -10 and 10

Introduction

The purpose of this lab is to learn how to operate a wind tunnel in order to measure the surface pressure of a two-dimensional NACA airfoil across various angles of incidence. This will help gain an understanding of how to compute lift and drag coefficients associated with the airfoil at different angles of incidence. Based on the thin airfoil theory's ability to accurately portray the behavior of the NACA 0012, it can be inferred that the data collected will match published data relating to the airfoil. The data that will be collected are the airfoil's angle of attack and the different pressures registered at each of the 16 pressure taps.

Data will be collected through the use of the pressure transducer, which will record pressures at distinct points on both the upper and lower surfaces of the airfoil. In addition, data from the wind tunnel and the 2D NACA 0012 airfoil will be collected. The airfoil has the ability to rotate, which enables adjustments to its attack angle. The NACA 0012, positioned within the wind tunnel, will undergo controlled rotations and data collection to help analyze the coefficients.

Each side of the airfoil has 9 pressure taps on both the upper and lower surfaces. These taps will be able to take measurements of the pressure across the airfoil's surface, which will be used for analysis. The free-stream velocity used throughout the experiment can be used to find the gauge pressure, which allows the calculation of the voltage needed to power the wind tunnel.
This free-stream velocity equation is:

$$V = \sqrt{\frac{2(P_{stag} - P_{static})}{\rho_{air}}} \qquad (1)$$

Where V is the free-stream velocity in the wind tunnel (10 m/s), P_{stag} is the stagnation pressure, P_{static} is the static pressure, and ρ_{air} is the density of air (1.169 kg/m^3). The ($P_{stag} - P_{static}$) can be substituted for $P_{gage,\ pressure\ gage}$, which can be calculated using

$$P_{gage} = C(V_{measured} - V_{offset}) \qquad (2)$$

Where C is the calibration constant 823 Pa/V of the pressure transducer, $V_{measured}$ is the measured voltage from the pressure transducer while the jet is on, and V_{offset} is the measured voltage at static conditions.

The conversion between psi and Pa is:

$$Pa = 6894.76 \times psi \qquad (3)$$

Using Equations (1) and (2) and converting the units, the equation to find the pressure coefficient:

$$C_p = \frac{(P - P_\infty)}{\frac{1}{2}\rho_{air} V_\infty^2} \qquad (4)$$

Where C_p is the pressure coefficient, ρ_{air} is the density of air V^2_∞ is the freestream velocity, and P - P_∞ is the pressure readings from the recorded data of the respective pressure tap, since the Scanivalve computes the difference between pressure on the airfoil and the pressure of the freestream velocity.

Once the P_{gage} is calculated, the lift and drag forces can be calculated:

$$\widehat{F_L} = \int_A P\widehat{dA} \qquad (5)$$

Where $\widehat{F_L}$ is the lift force, P is the pressure, and $\widehat{dA}$ is the magnitude of dA (using the flat plate theory on the airfoil). With the angles of attack, the equations become

$$F_L = \int_A P \times cos(\alpha)\, dA \qquad (6)$$

This integral can be split into two, so one calculates the lower half and the other calculates the upper half

$$F_L = \int_{c,lower} Pcos(\alpha)dc - \int_{c,upper} Pcos(\alpha)dc \qquad (7)$$

Now the trapezoidal integration can be applied

$$F_L = \sum_{lower} \frac{(P-P_\infty)_i+(P-P_\infty)_{i+1}}{2}(C_{i+1}-C_i)cos(\alpha) - \sum_{upper} \frac{(P-P_\infty)_i+(P-P_\infty)_{i+1}}{2}(C_{i+1}-C_i)cos(\alpha) \quad (8)$$

Where C is the chord length. The drag force can be derived in a similar way; however, the difference would be to change cos(α) to sin(α), since the drag force is perpendicular to the lift force.

$$F_L = \sum_{lower} \frac{(P-P_\infty)_i+(P-P_\infty)_{i+1}}{2}(C_{i+1}-C_i)sin(\alpha) - \sum_{upper} \frac{(P-P_\infty)_i+(P-P_\infty)_{i+1}}{2}(C_{i+1}-C_i)sin(\alpha) \quad (9)$$

Like before, the $P–P_\infty$ can be substituted for the pressure readings.

Once the lift and drag forces have been found, they can be used to find their coefficients using the following equations.

$$F_L = \frac{1}{2}\rho_{air}V_\infty^2 S C_L$$
$$C_L = \frac{F_L}{\frac{1}{2}\rho_{air}V_\infty^2 S} \quad (10)$$

$$F_D = \frac{1}{2}\rho_{air}V_\infty^2 S C_D$$
$$C_D = \frac{F_D}{\frac{1}{2}\rho_{air}V_\infty^2 S} \quad (11)$$

Where F_L is the lift force, F_D is the drag force, ρ_{air} is the density of air (1.169 kg/m^3), V^2_∞ is the freestream velocity, S is the wing area, C_L is the coefficient of lift, and C_D is the coefficient of drag. Another equation for the coefficient of lift using the thin airfoil theory is, (Anderson, 352)

$$C_L = 2\pi\alpha \quad (12)$$

Experimental Setup

A two-dimensional NACA 0012 airfoil is positioned in the center of the test section of the wind tunnel, shown in Figure 1. The airfoil has 16 pressure taps total that are placed along both sides of the airfoil, 9 on top and 9 on bottom, with the leading edge and trailing edge sharing a point. Each pressure tap is located at a different x/c location as depicted in Figure 2. The pressure taps are used to send a signal to a pressure transducer in order to collect data. The pressure transducer used in this experiment is a Scanivalve DSA3217, it is connected to a program called ScanTel that collects data in units of psi



Figure 1. NACA 0012 Airfoil in Test Section of Wind Tunnel

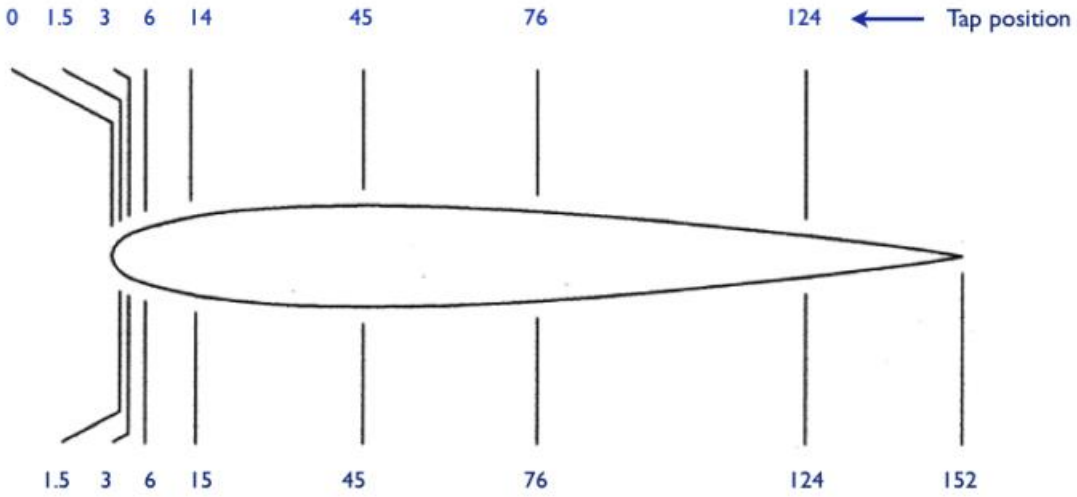


Figure 1. NACA 0012 Pressure Tap Distribution.

Table 1: Pressure Tap Position Along the Chord and Pressure Tap Number

Top	0 1	1.5 mm 9	3 mm 10	6 mm 11	14 mm 12	45 mm 13	76 mm 14	124 mm 15	152 mm 16
Bottom	0 1	1.5 2	3 3	6 4	15 5	45 6	76 7	124 8	152 16

Figure 2. x Positions of Pressure Taps

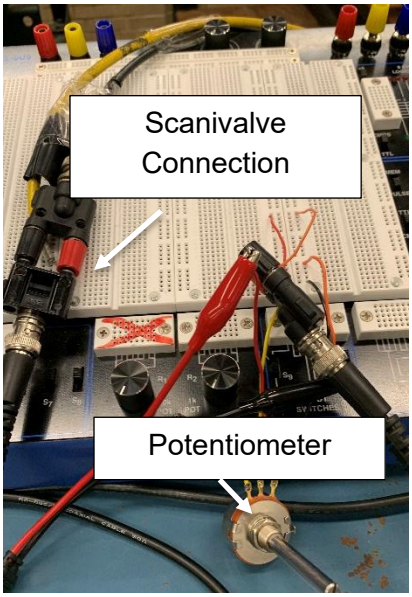


Figure 3 Scanivalve Power Connection

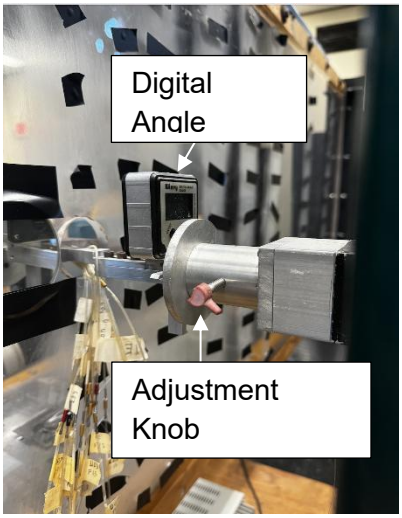


Figure 4. Attack Angle Adjustment

Before beginning the experiment, the voltage required to power the wind tunnel at a speed of 10 m/s needs to be determined. This process begins by recording the V_{off} of the wind tunnel as well as a set of offset pressure readings. V_{off} is found to be 2.5720 V by using MATLAB's mean function. Then the potentiometer was used to change the wind tunnel speed to around 10 m/s by using a MATLAB script to check both the velocity and voltage used, which was 10.0362 m/s at 2.6235 V.

Once the velocity is consistent, the airfoil's angle of attack can then be changed and its data collected on the Scanivalve. The angles of attack were controlled and changed by using an adjustable knob and a digital angle reader, shown in Figure 4. Data were recorded at angles of -10, -6, -3, 0, 3, 6, 10, 15, 20 degrees.

Results

The data acquired using Scantily, initially in psi, were averaged and then subtracted by the pressure data collected when the wind tunnel was off (Data Table 1). Once subtracted, these values were converted to Pa using Equation (3) before continuing to find the coefficients of pressure, lift, and drag using Equations (4), (10), and (11), respectively.

	Pressure Tap Point (psi)															
(Angle of Attack)	0	1	2	3	4	5	6	7	8	9	10	11	12	13	14	15
-10	-1.11 E-02	-3.27 E-02	-2.91 E-02	-2.49 E-02	-2.35 E-02	-1.11 E-02	-7.19 E-03	-5.63 E-03	-3.78 E-03	-6.36 E-03	-4.00 E-03	-8.08 E-04	-2.47 E-03	-3.19 E-03	-3.28 E-03	-3.25 E-03
-6	-7.78 E-04	-1.77 E-02	-1.90 E-02	-1.95 E-02	-1.54 E-02	-1.14 E-02	-6.40 E-03	-5.45 E-03	-5.84 E-03	-5.66 E-03	-1.28 E-03	-1.76 E-03	-3.78 E-03	-4.06 E-03	-3.55 E-03	-2.89 E-03
-3	4.30 E-03	-6.94 E-03	-1.06 E-02	-1.45 E-02	-1.23 E-02	-8.91 E-03	-6.35 E-03	-5.70 E-03	-5.39 E-03	-3.50 E-03	-1.56 E-03	-3.99 E-03	-4.80 E-03	-4.59 E-03	-3.72 E-03	-2.94 E-03
0	6.02 E-03	5.41 E-04	-3.87 E-03	-1.01 E-02	-9.30 E-03	-7.65 E-03	-5.34 E-03	-5.04 E-03	-2.48 E-03	-1.07 E-04	-4.85 E-03	-6.36 E-03	-5.82 E-03	-5.11 E-03	-4.02 E-03	-3.58 E-03
3	5.54 E-03	5.37 E-03	1.74 E-03	-5.58 E-03	-6.07 E-03	-6.12 E-03	-4.30 E-03	-3.99 E-03	-3.66 E-03	-5.73 E-03	-9.13 E-03	-9.34 E-03	-7.07 E-03	-5.91 E-03	-4.84 E-03	-3.64 E-03
6	2.07 E-03	6.47 E-03	5.16 E-03	-2.14 E-03	-3.46 E-03	-4.81 E-03	-3.58 E-03	-3.63 E-03	-1.23 E-02	-1.27 E-02	-1.37 E-02	-1.23 E-02	-8.25 E-03	-7.20 E-03	-4.39 E-03	-2.65 E-03
10	-7.19 E-03	4.45 E-03	6.89 E-03	1.51 E-03	-3.90 E-04	-3.13 E-03	-2.59 E-03	-3.22 E-03	-2.69 E-02	-2.35 E-02	-1.92 E-02	-1.75 E-02	-9.02 E-03	-6.95 E-03	-4.83 E-03	-2.56 E-03
15	-3.87 E-03	4.88 E-03	6.87 E-03	1.93 E-03	1.47 E-04	-3.00 E-03	-3.00 E-03	-4.41 E-03	-1.49 E-02	-1.11 E-02	-1.04 E-02	-1.11 E-02	-1.04 E-02	-1.03 E-02	-9.24 E-03	-6.92 E-03

Data Table 1.

Data Table 2 shows the coefficients of pressure for each pressure tap at each angle of attack used during the performance of the experiment. These values, along with the x location given in

Figure 2, were used in order to create graphs of C_P vs x/c, where x/c was found by dividing the x value of the pressure taps by the chord length.

	Coefficient of Pressure															
(Angle of Attack)	0	0.0098684210533	0.0197368421	0.0394736842105	0.0986842105316	0.296052631579	0.5	0.815789473684	0.0098684210533	0.0197368421	0.0394736842105	0.0921052631579	0.296052631579	0.5	0.815789473684	1
-10	-1.81E+00	-5.33E+00	-4.74E+00	-4.05E+00	-3.83E+00	-1.81E+00	-1.17E+00	-9.15E-01	6.15E-01	1.03E+00	6.50E-01	1.31E-01	-4.02E-01	-5.19E-01	-5.34E-01	-5.28E-01
-6	-1.27E-01	-2.88E+00	-3.09E+00	-3.16E+00	-2.51E+00	-1.86E+00	-1.04E+00	-8.86E-01	9.51E-01	9.21E-01	2.08E-01	-2.87E-01	-6.14E-01	-6.60E-01	-5.78E-01	-4.70E-01
-3	6.99E-01	-1.13E+00	-1.72E+00	-2.36E+00	-2.00E+00	-1.45E+00	-1.03E+00	-9.28E-01	8.76E-01	5.69E-01	-2.54E-01	-6.50E-01	-7.81E-01	-7.47E-01	-6.05E-01	-4.79E-01
0	9.79E-01	8.80E-02	-6.30E-01	-1.64E+00	-1.51E+00	-1.24E+00	-8.68E-01	-8.19E-01	4.04E-01	-1.75E-02	-7.88E-01	-1.03E+00	-9.47E-01	-8.31E-01	-6.54E-01	-5.83E-01
3	9.01E-01	8.74E-01	2.84E-01	-9.08E-01	-9.87E-01	-9.96E-01	-6.99E-01	-6.49E-01	-5.95E-01	-9.32E-01	-1.48E+00	-1.52E+00	-1.15E+00	-9.61E-01	-7.88E-01	-5.93E-01
6	3.37E-01	1.05E+00	8.40E-01	-3.49E-01	-5.62E-01	-7.83E-01	-5.83E-01	-5.90E-01	-1.99E+00	-2.07E+00	-2.23E+00	-2.01E+00	-1.34E+00	-1.17E+00	-7.14E-01	-4.31E-01
10	-1.17E+00	7.24E-01	1.12E+00	2.45E-01	-6.34E-02	-5.09E-01	-4.21E-01	-5.24E-01	-4.37E+00	-3.82E+00	-3.13E+00	-2.85E+00	-1.47E+00	-1.13E+00	-7.86E-01	-4.17E-01
15	-6.29E-01	7.94E-01	1.12E+00	3.13E-01	2.40E-02	-4.88E-01	-4.88E-01	-7.18E-01	-2.42E+00	-1.81E+00	-1.69E+00	-1.81E+00	-1.70E+00	-1.68E+00	-1.50E+00	-1.13E+00
20	-8.78E-01	5.67E-01	1.11E+00	4.85E-01	2.09E-01	-3.96E-01	-4.84E-01	-8.20E-01	-1.92E+00	-1.56E+00	-1.55E+00	-1.66E+00	-1.61E+00	-1.66E+00	-1.63E+00	-1.55E+00

Data Table 2.

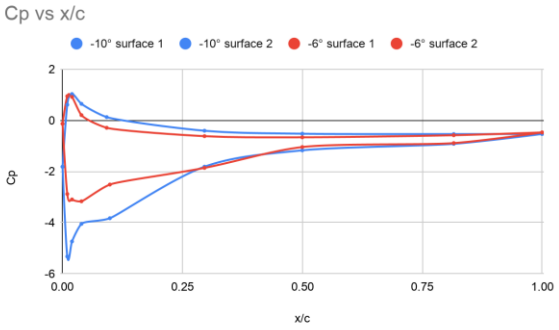


Figure 5. C_P vs x/c (α = -10, -6)

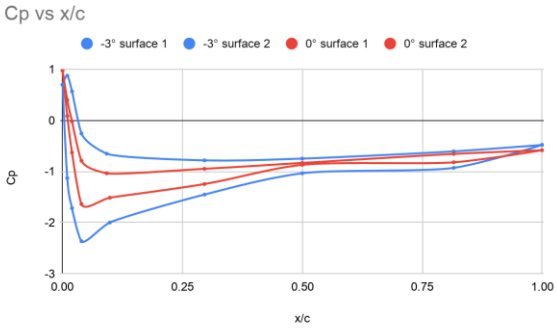


Figure 6. C_P vs x/c (α = -3, 0)

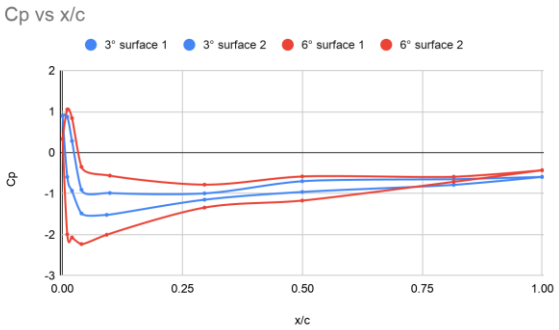


Figure 7. C_P vs x/c (α = 3, 6)

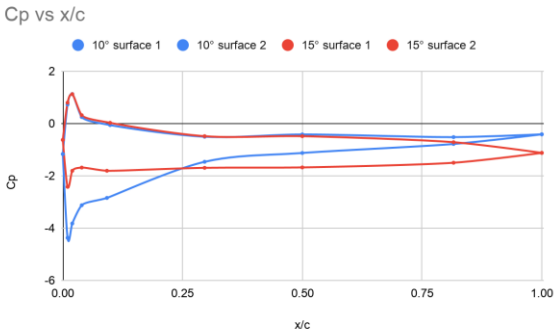


Figure 8. C_P vs x/c (α = 10, 15)

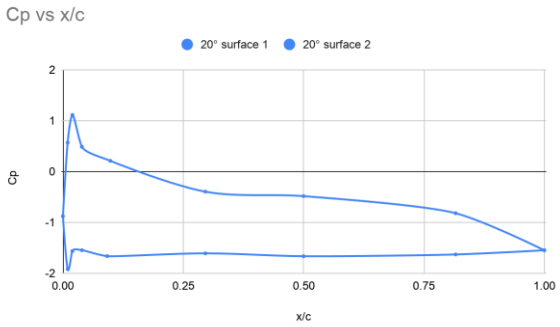


Figure 9. C_P vs x/c (α = 20)

Using Equations (10) and (11), the coefficients of lift and drag were calculated. The computed values were then plotted against the various angles of attack (Figure 10), to then be compared to a graph that uses values of C_L from Equation (12)

	Sum of C_L and C_D								
Angle of attack (α)	-10	-6	-3	0	3	6	10	15	20
C_L	-1.35996	-0.93310	-0.59688	-0.21714	0.25594	0.62243	1.03436	1.09981	1.06851
$C_{D,P}$	0.23980	0.09807	0.03128	0.00000	0.01341	0.06542	0.18239	0.29469	0.38891

Data Table 3.

	Thin Airfoil Theory								
Angle of attack (deg)	-10	-6	-3	0	3	6	10	15	20
C_L	-1.0966	-0.6580	-0.3290	0.0000	0.3290	0.6580	1.0966	1.6449	2.1932

Data Table 4.

Data Table 3 shows the calculated values of C_L and C_D using Equations (10) and (11), whereas Data Table 4 shows the values of C_L using the thin airfoil theory (Equation 12)

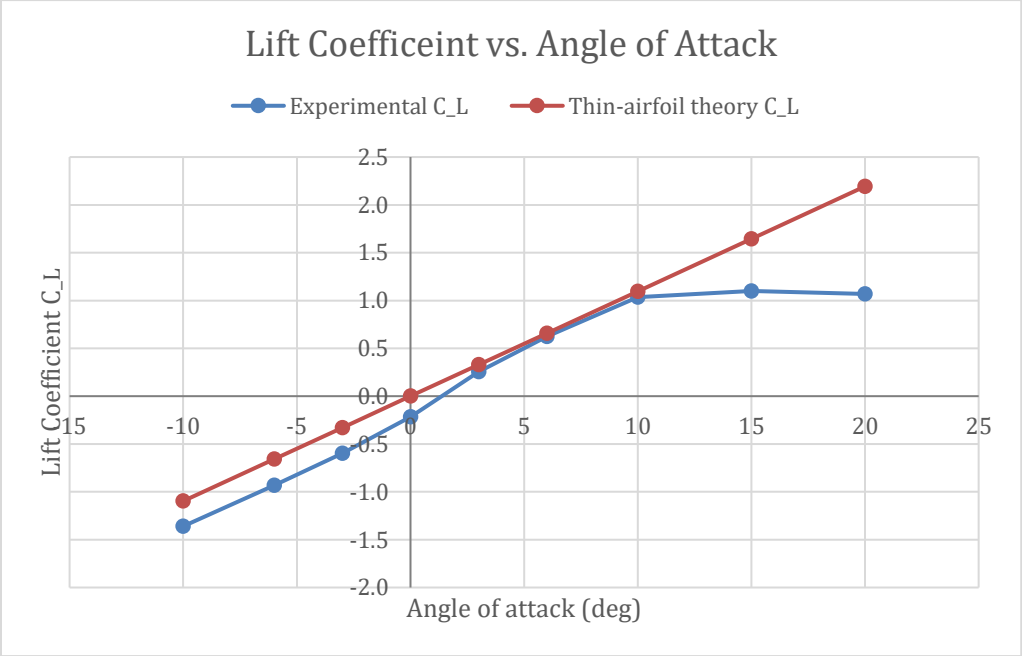


Figure 10. C_L vs α for Experimental Data and Thin Airfoil Theory

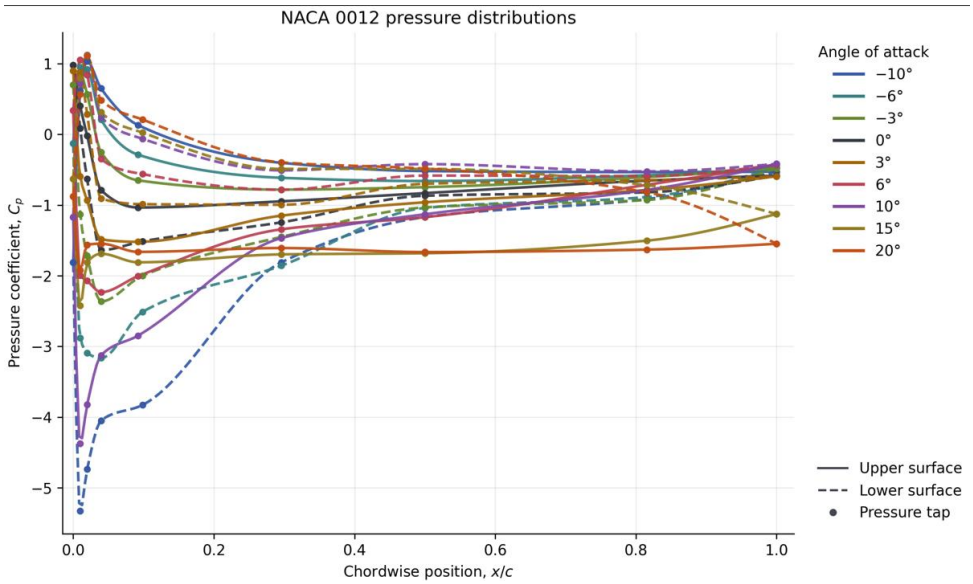


Figure 11. C_P vs All Alpha

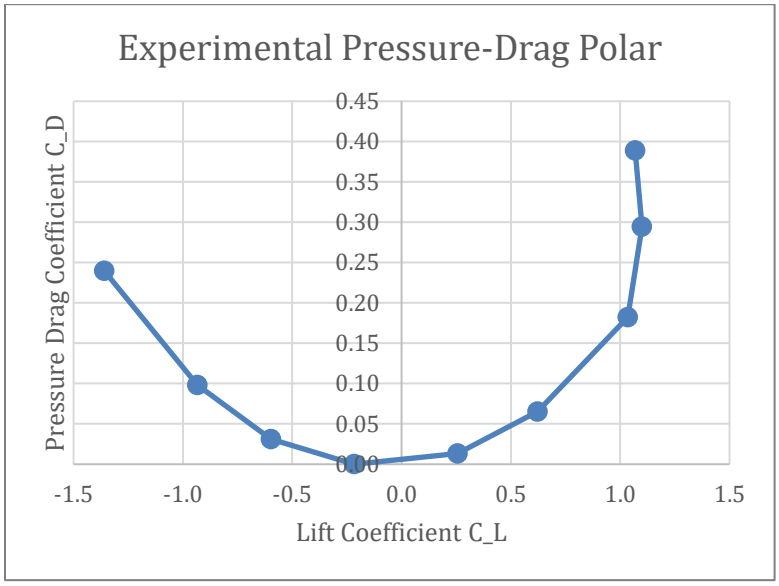


Figure 12. C_D vs C_L

Figures 13, 14, and 15 are used to compare the calculated/experimental data for the coefficients of drag, lift, and pressure versus the actual values the Turbulence Modeling Resource has calculated and plotted.

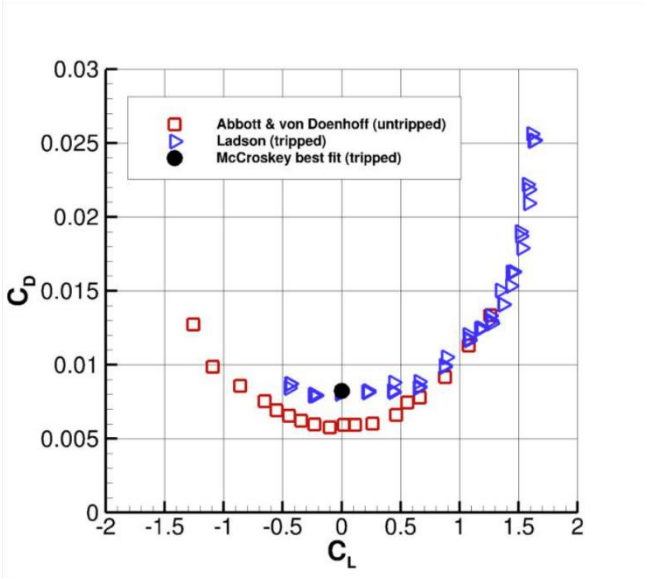


Figure 13. C_L vs. C_D -TMR

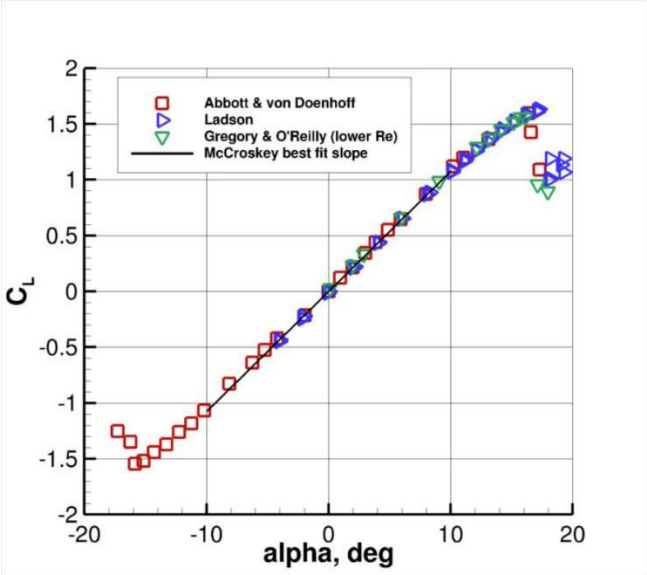


Figure 14. C_L vs Alpha -TMR

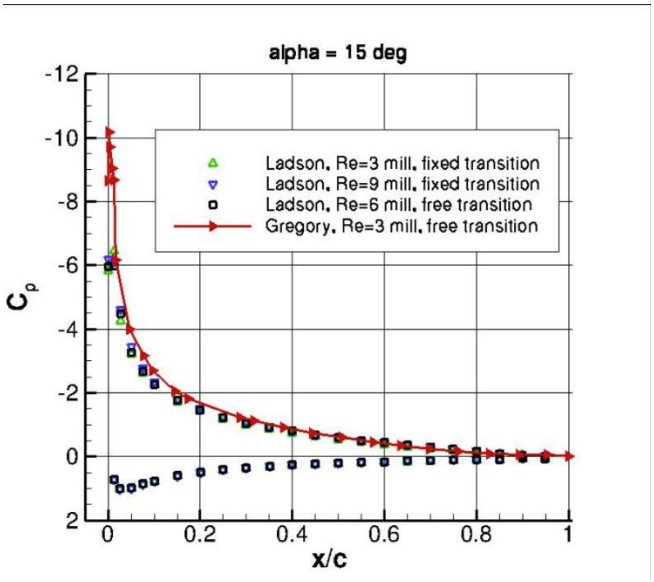


Figure 15. C_P vs x/c -TMR

Discussion of Results

During the analysis of the coefficient of pressure of the NACA 0012 airfoil at a freestream velocity of 10 m/s, it was found that the coefficient of pressure was at its lowest at an attack angle of 10°. This can be seen in Figure 10, as the thin airfoil theory starts to differ from that point. Similarly, in Figures 5 through 9, the ending coefficient starts to drift from 0 down to a negative value at an attack angle of 10°. It can also be seen that Figure 15 and Figure 11 have the same relationship but are inverses of each other. It can also be said that the experimental data follow the same trend as the empirical data while having a few minor differences that could be caused by errors while conducting the experiment. This can be seen when looking at the amplitudes of both graphs; the range of the empirical data goes from about -10 to 2, while the experimental data goes from about -6 to 1. In Figures 14 and Figure 10, the graphs of C_L vs Alpha, it can be seen that the experimental data closely relates to the empirical data until the angle of 10°. Figure 14 depicts the values of C_L calculated by the use of TMR; this graph shows the $C_{L,max}$ to be 17°, whereas Figure 10, using experimental data, shows $C_{L,max}$ to be at 15°. Both sets of data show the stall angle, alpha at $C_{L,max}$, to be at different points. Although this deviation occurred, this deviation occurred, the thing airfoil theory was still proved to be accurate until the angle of 10° when stall occurred.

While analyzing the experimental data collected for the coefficients of lift and drag (Figure 12) along with the empirical data from Figure 13, it can be seen that both sets of data deviate the most from each other when the attack angle reaches 15°. The experimental values are also shifted down compared to the empirical data. It can also be observed that there was more drag on the airfoil during the experiment than was expected to be based on the empirical data.

A source of deviation could be the viscous effects and separation of the flow from the airfoil (Anderson, 69, 392). This separation causes drag due to pressure, which would explain why the drag coefficient of the experimental data was higher than the empirical data found them to be. Another source of error can be a result of not being able to accurately estimate the exact voltage needed to power the wind tunnel to a velocity of 10 m/s, which could have resulted in the wind tunnel having a velocity higher or lower than 10 m/s.

Conclusions

The NACA 0012 airfoil reaches $C_{L,max}$ at an attack angle of 15°, which can be seen in Figure 10, where it then begins to stall, resulting in a decrease of performance as shown in Figure 11. However, this observation does not match that of the published data from TMR. The TMR data says the airfoil starts to stall at 17°. This error could be due to sources of error such as the effects of viscosity and the inconsistencies of the Scanivale and ScanTel. However, despite a change in values, both data collections follow a similar behavior.

References

Anderson, J.D.A, (2017). Fundamentals of Aerodynamics Sixth edition, Section 4.7: Classical Thin Airfoil Theory: The Symmetric Airfoil | New York, NY: McGraw-Hill Education, [2017]. (Pg. 352)

2D NACA 0012 airfoil validation. (2016). Github.Io. https://tmbwg.github.io/turbmodels/naca0012_val.html